

Capacitor Bank Protection via Constraint WLS Dynamic State Estimation Method (CWLS-DSE)

Liangyi Sun, *Student Member, IEEE*, Rui Fan, *Student Member, IEEE*, A. P. Sakis Meliopoulos, *Fellow, IEEE*,
Yu Liu, *Student Member, IEEE*, and Zhenyu Tan, *Student Member, IEEE*
School of Electrical and Computer Engineering, Georgia Institute of Technology, USA
Email: lsun30@gatech.edu

Abstract- A dynamic state estimation (DSE) based protection algorithm using weighted least square (WLS) method was introduced recently. In this paper, the DSE-based protection algorithm using constraint weighted least squares (CWLS) method is applied to capacitor bank protection. This approach monitors the health status of the capacitor bank by fitting real time measurements to the capacitor bank dynamic model via dynamic state estimation. Virtual measurements are added to the measurements set by considering the physical laws that must be obeyed by the capacitor bank (i.e. KVL, KCL). Virtual measurements can be handled as measurements with high accuracy or as constraints to the dynamic state estimation. The CWLS method treats the virtual measurements as constraints while the WLS method treats them as highly accuracy measurements. Comparison of capacitor bank protection results using unconstraint WLS and CWLS is provided. It is shown that the proposed method can detect internal faults and issue the trip signal correctly. The use of CWLS provides a more sensitive protection for capacitor banks.

Index Terms- Dynamic state estimation, constraint weight least squares, dynamic model, power system protection

I. INTRODUCTION

SHUNT capacitor banks are widely utilized in power systems for power factor correction and voltage support, and thereby improving the overall power transmission efficiency [1]. With more distributed generation connecting to power grid in the future, capacitor banks will definitely play a more important role in the distribution network. Loss of capacitor banks could result in voltage drop at the bank terminal and affects the balance of the grid [2]. Thus a reliable and secure protection scheme for capacitor banks is critical for the proper operation of the power grid. However, the increasing complexity of capacitor bank configurations makes it difficult to find one general protection method for all configurations and sensitive enough to detect all possible faults. Even for one specific capacitor bank configuration, there is still no universal relaying method which could detect all the faults inside the capacitor bank [3]. Due to the complicated physical arrangements of large capacitor banks, failures of individual capacitor units may not be detected by the traditional protective relaying schemes. According to the newest IEEE C37.99 *Draft Guide for the Protection of Shunt*

Capacitor Banks, 2012, different unbalance relaying methods are introduced for different bank connections. A review of existing common capacitor bank protection approaches is given in [2]. Each of the protection methods introduced in [2] has some major disadvantages (too sensitive, no indication of faulted phase, masks balanced failures, high cost, etc.) which could risk the availability and safety of capacitor banks. Many research efforts have been carried out on improving or creating new capacitor bank protection methods, examples are listed in [4]-[6]. Improved overvoltage protection of capacitor banks is introduced in [4]. MOV arresters are applied to three phase capacitor banks to provide overvoltage protection. The stresses on MOV arresters are greatly different for different configuration. Choosing the proper arresters requires significant studies. [5] and [6] show an improved overcurrent protection of capacitor banks. This scheme can better discriminate between faults and switching inrush currents. A table is given in [5] to guide the users for the correct overcurrent relay settings. Relay settings for capacitor bank overcurrent protection is a compromise among conflicting factors.

The purpose of this paper is to introduce an innovative Dynamic State Estimation (DSE) based protection of capacitor bank using the constraint weighted least squares (CWLS) method, which is applicable to any capacitor bank configuration and covers all fault conditions. It can be implemented in microprocessor relays, thus utilizing the full potential of microprocessor's computation capability. The DSE-based protection scheme for capacitor banks is based on performing state estimation by using capacitor bank dynamic model. It gathers the real-time data from the capacitor bank and tries to fit the real-time measurements to the bank dynamic measurement model. Any internal abnormality that causes bank configuration changes would be manifested as deviations of the measurements from the dynamic model predicted values. On the other hand, any external fault or switching inrush current that do not change the bank structure would not influence the results of dynamic state estimation. Hence, the DSE-based protection of capacitor banks detects any type of internal fault for all

bank configurations without any specific settings and coordination with other relays.

As mentioned above, the CWLS method is utilized during the dynamic state estimation in the paper. The capacitor bank virtual measurements which are the capacitor bank internal dynamic equations, that represent physical laws (i.e. Kirchhoff Current Law and Kirchhoff Voltage Law), are treated as constraints. The reason why unconstrained weighted least squares (WLS) is not utilized here is because WLS tries to find the best estimate for the states that generate the minimum weighted squared error and it works well with a measurement set that represents actual measurements with usual measurement errors but when it is used to handle virtual measurements with very small uncertainty, it may generate numerical instabilities due to the large separation between the variances of the actual measurements and the virtual measurements.

The CWLS method was first formulated by Phillips [7]. CWLS method formulates an optimization problem subject to equality constraints. The Lagrange function with the enforcement of equality constraints is used in CWLS to reach a solution using an augmented set of Normal Equations. The method of Lagrange multipliers is used to solve the optimization problem defined as a constraint state estimation problem.

The organization of this paper is as follows. In Section II, the derivation of capacitor bank dynamic measurement model is described. In Section III, DSE-based protection using CWLS method is introduced. In Section IV, results of the DSE-based protection using WLS and CWLS are compared. Section V presents conclusions.

II. DERIVATION OF CAPACITOR BANK DYNAMIC MEASUREMENT MODEL

A. Capacitor Bank Dynamic Quadratized Model

A capacitor bank dynamic mathematical model is derived from its physical circuit. This model is a set of differential and algebraic equations. A capacitor bank consists of hundreds of capacitor cans and each can has several capacitor elements. The circuit model of one capacitor is shown in Figure 1.

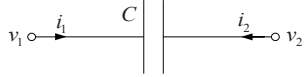


Figure 1. Circuit model of one capacitor
The mathematical model of the above circuit is:

$$\begin{aligned} i_1(t) &= C \cdot \frac{d}{dt}(v_1(t) - v_2(t)) \\ i_2(t) &= C \cdot \frac{d}{dt}(v_2(t) - v_1(t)) \end{aligned} \quad (1)$$

By adding up all the equations of the capacitor elements in the capacitor bank according to their connections, the capacitor bank dynamic model is obtained. In general, any device can be modeled in this way. A general form of a device model is shown here to make the proposed algorithm object-oriented. Any higher order nonlinearities can be

reduced to second order by introducing additional variables. This model is referred to as dynamic quadratized device model (QDM):

$$\begin{aligned} i(t) &= Y_{eqx1} \mathbf{x}(t) + D_{eqxd1} \frac{d\mathbf{x}(t)}{dt} + C_{eqc1} \\ 0 &= Y_{eqx2} \mathbf{x}(t) + D_{eqxd2} \frac{d\mathbf{x}(t)}{dt} + C_{eqc2} \\ 0 &= Y_{eqx3} \mathbf{x}(t) + \left\{ \mathbf{x}(t)^T \left\langle \begin{array}{c} \vdots \\ F_{eqx3}^i \\ \vdots \end{array} \right\rangle \mathbf{x}(t) \right\} + C_{eqc3} \end{aligned} \quad (2)$$

where, matrices Y are linear term coefficients, matrices D are linear differential term coefficients, matrices F are quadratic term coefficients, vectors C are constants, vector \mathbf{x} is the state variables, vector i is terminal currents and (t) stands for time stamp t (other time stamps will be introduced later in the paper).

The QDM has three sets of equations. The first set represents the interface equations, which expresses the through variables as functions of the device state. The second and third sets are linear and nonlinear internal equations, respectively, of the protection zone. The capacitor bank model is linear and the third set of equations is null in this case. However, we keep these equations for the purpose of presenting the method in its most general form.

B. Dynamic AQCF Device Model

Quadratic integration method is used to convert the QDM to the algebraic quadratic companion form (AQCF). Quadratic integration is based on a numerical integration scheme that assumes the model states vary quadratically within a time step h [8]. The values of currents and states at time stamp t_m (intermediate time stamp of t and $t-h$) and $t-h$ are introduced by this integration method. The AQCF device model, which is the result of applying quadratic integration, is shown below directly due to the space limitation:

$$\begin{aligned} \begin{pmatrix} i(t) \\ 0 \\ 0 \\ i(t_m) \\ 0 \\ 0 \end{pmatrix} &= Y_{eqx} \mathbf{x}(t, t_m) + \left\{ \mathbf{x}(t, t_m)^T \left\langle \begin{array}{c} \vdots \\ F_{eqx}^i \\ \vdots \end{array} \right\rangle \mathbf{x}(t, t_m) \right\} + C_{eq} \\ C_{eq} &= N_{eqx} \mathbf{x}(t-h) + M_{eq} i(t-h) + K_{eq} \end{aligned} \quad (3)$$

where: $i(t)$, $i(t_m)$ are currents that flow into the device at two adjacent time instances time t and time t_m ; $\mathbf{x}(t)$, $\mathbf{x}(t_m)$ are state variables of the AQCF device model at time t and time t_m ; Y_{eqx} is linear term coefficients; F_{eqx} is quadratic term coefficients; C_{eq} is past history part; N_{eqx} is past history linear term coefficients; M_{eq} is past history current term coefficients; K_{eq} is past history constants.

$$Y_{eqx} = \begin{bmatrix} \frac{4}{h}D_{eqxd1} + Y_{eqx1} & -\frac{8}{h}D_{eqxd1} \\ \frac{4}{h}D_{eqxd2} + Y_{eqx2} & -\frac{8}{h}D_{eqxd2} \\ Y_{eqx3} & 0 \\ \frac{1}{2h}D_{eqxd1} & \frac{2}{h}D_{eqxd1} + Y_{eqx1} \\ \frac{1}{2h}D_{eqxd2} & \frac{2}{h}D_{eqxd2} + Y_{eqx2} \\ 0 & Y_{eqx3} \end{bmatrix} \quad K_{eq} = \begin{bmatrix} 0 \\ 0 \\ C_{eqc3} \\ \frac{3}{2}C_{eqc1} \\ \frac{3}{2}C_{eqc2} \\ C_{eqc3} \end{bmatrix}$$

$$N_{eqx} = \begin{bmatrix} -Y_{eqx1} + \frac{4}{h}D_{eqxd1} \\ -Y_{eqx2} + \frac{4}{h}D_{eqxd2} \\ 0 \\ \frac{1}{2}Y_{eqx1} - \frac{5}{2h}D_{eqxd1} \\ \frac{1}{2}Y_{eqx2} - \frac{5}{2h}D_{eqxd2} \\ 0 \end{bmatrix} \quad F_{eqx} = \begin{bmatrix} 0 & 0 \\ 0 & 0 \\ F_{eqxc3} & 0 \\ 0 & 0 \\ 0 & 0 \\ 0 & F_{eqxc3} \end{bmatrix} \quad M_{eq} = \begin{bmatrix} I_{size(i(t))} \\ 0 \\ 0 \\ \frac{1}{2}I_{size(i(t))} \\ 0 \\ 0 \end{bmatrix}$$

It should be apparent that the AQCF device model is dynamic and it represents the transients (dynamics) of the protection zone.

C. Dynamic AQCF Measurement Model

Measurement model is just the mathematical expression of each measurement as a function of state variables. Four types of measurements are considered in this paper: actual measurements, pseudo measurements, derived measurements and virtual measurements.

The **actual measurement** is a measurement obtained by available metering devices. It has error due to the data acquisition system. The **pseudo measurement** is not a real measurement but its value can be approximately known without metering, like the neutral voltage. Since the value of the pseudo measurement is not precise, it is considered to have big error. The **derived measurement** is not a real measurement but its value can be derived from available actual measurements. This measurement has the same noise as the actual one. The **virtual measurement** is not a real measurement neither, but represents a physical law, for example, the internal equations (equations with zero on the left) of the AQCF model. Virtual measurements are noiseless, if it is assumed that the model is accurate.

In summary, all measurements can be stacked together and be written in a common syntax, referred to as the AQCF measurement model.

$$\mathbf{h}_{all}(\mathbf{x}) = Y_z \mathbf{x}(t, t_m) + \begin{Bmatrix} \vdots \\ \mathbf{x}(t, t_m)^T \langle F_z^i \rangle \mathbf{x}(t, t_m) \\ \vdots \end{Bmatrix} \quad (4)$$

$$+ N_z \mathbf{x}(t-h) + M_z i(t-h) + K_z$$

If the virtual measurements are listed separately, equation (4) would be separated as:

$$\mathbf{h}_{nonVirtual}(\mathbf{x}) = Y_{z1} \mathbf{x}(t, t_m) + \begin{Bmatrix} \vdots \\ \mathbf{x}(t, t_m)^T \langle F_{z1}^i \rangle \mathbf{x}(t, t_m) \\ \vdots \end{Bmatrix}$$

$$+ N_{z1} \mathbf{x}(t-h) + M_{z1} i(t-h) + K_{z1} \quad (5)$$

$$0 = \mathbf{g}(\mathbf{x}) = Y_{z2} \mathbf{x}(t, t_m) + \begin{Bmatrix} \vdots \\ \mathbf{x}(t, t_m)^T \langle F_{z2}^i \rangle \mathbf{x}(t, t_m) \\ \vdots \end{Bmatrix}$$

$$+ N_{z2} \mathbf{x}(t-h) + M_{z2} i(t-h) + K_{z2}$$

where: $h(x)$ is the measurements (actual, pseudo, derived and virtual measurements) at two adjacent time instances time t and time t_m ; $x(t)$, $x(t_m)$ are state variables at time t and time t_m ; Y_z , Y_{z1} , Y_{z2} are matrices of linear term coefficients; F_z , F_{z1} , F_{z2} are matrices of quadratic term coefficients; N_z , N_{z1} , N_{z2} are matrices of past history linear term coefficients; M_z , M_{z1} , M_{z2} are matrices of past history current term coefficients; K_z , K_{z1} , K_{z2} are matrices of past history constants.

The AQCF measurement model still contains all the characteristics of the AQCF device model, thus it represents the transients of the protection zone. This dynamic AQCF measurement model is utilized for the DSE-based protection.

II. DYNAMIC STATE ESTIMATION-BASED PROTECTION USING CONSTRAINT WLS METHOD

This section presents the proposed constraint WLS method. In this section, we first show the WLS method [9]-[11] and CWLS methods and then its application to the DSE-based protection:

A. Unconstraint WLS method

WLS method tries to find the best estimate for the states that generate the minimum weighted squared error. The optimization problem using dynamic AQCF measurement model in equation (4) is:

$$\text{Minimize } J = \sum_i \left(\frac{h_{all,i}(\mathbf{x}) - z_i}{\sigma_i} \right)^2 = \sum_i s_i^2 = \boldsymbol{\eta}^T W \boldsymbol{\eta} \quad (6)$$

where: $s_i = \frac{\eta_i}{\sigma_i}$, $W = \text{diag} \left\{ \dots, \frac{1}{\sigma_i^2}, \dots \right\}$, z_i is the measurement

data. σ_i is standard deviation of each measurement, which is the noise in the meter (a very tiny noise is added to the virtual measurement to make the algorithm work) and W is the diagonal matrix whose diagonal non-zero entries are the inverse of the variance of the measurement standard deviation.

The solution is given with the Newton's iterative algorithm:

$$\mathbf{x}^{\nu+1} = \mathbf{x}^\nu - (H^T W H)^{-1} H^T W (\mathbf{h}_{all}(\mathbf{x}^\nu) - \mathbf{z}) \quad (7)$$

where H is the Jacobean matrix:

$$H = \frac{\partial \mathbf{h}_{all}(\mathbf{x})}{\partial \mathbf{x}} = Y_{m,x} + \begin{Bmatrix} \vdots \\ \mathbf{x}^T F_{m,x}^i + F_{m,x}^i \mathbf{x} \\ \vdots \end{Bmatrix} \quad (8)$$

The covariance matrix of the state is:

$$\text{Cov}(\mathbf{x}) = (H^T W H)^{-1} \quad (9)$$

B. Constraint WLS method

The virtual measurements are treated as constraints in the CWLS method. The optimization problem using dynamic AQCF measurement model in equation (5) is:

$$\text{Minimize } J = \sum_{i=1}^n \left(\frac{h_{nonVirtual,i}(\mathbf{x}) - z_i}{\sigma_i} \right)^2 = \sum_{i=1}^n s_i^2 = \boldsymbol{\eta}^T W \boldsymbol{\eta} \quad (10)$$

Subject to:

$$0 = \mathbf{g}(\mathbf{x}) = Y_{z2} \mathbf{x}(t, t_m) + \begin{Bmatrix} \vdots \\ \mathbf{x}(t, t_m)^T \langle F_{z2}^i \rangle \mathbf{x}(t, t_m) \\ \vdots \end{Bmatrix} \quad (11)$$

$$+ N_{z2} \mathbf{x}(t-h) + M_{z2} i(t-h) + K_{z2}$$

The method of Lagrange multipliers is applied here. A new variable $\boldsymbol{\lambda}$ called a Lagrange multiplier is introduced and the Lagrange function is defined as follows:

$$L(\mathbf{x}, \boldsymbol{\lambda}) = J + \boldsymbol{\lambda}^T \mathbf{g}(\mathbf{x}) \quad (12)$$

The necessary conditions for the Lagrange function are:

$$\frac{\partial L(\mathbf{x}, \boldsymbol{\lambda})}{\partial \mathbf{x}} = (\mathbf{h}_{nonVirtual}(\mathbf{x}) - \mathbf{z})^T W \frac{\partial \mathbf{h}_{nonVirtual}(\mathbf{x})}{\partial \mathbf{x}} + \boldsymbol{\lambda}^T \frac{\partial \mathbf{g}(\mathbf{x})}{\partial \mathbf{x}} = 0 \quad (13)$$

$$\frac{\partial L(\mathbf{x}, \boldsymbol{\lambda})}{\partial \boldsymbol{\lambda}} = \mathbf{g}(\mathbf{x}) = 0$$

The solution of above equations could be obtained iteratively by Newton's iterative method with an initial guess \mathbf{x}_0 and $\boldsymbol{\lambda}_0$. The update is given by:

$$\mathbf{x}^{v+1} = \mathbf{x}^v + \Delta \mathbf{x} \quad (14)$$

$$\boldsymbol{\lambda}^{v+1} = \boldsymbol{\lambda}^v + \Delta \boldsymbol{\lambda}$$

Use the Taylor expansion at $v+1$ iteration and ignore the second or higher order terms.

$$\mathbf{h}_{nonVirtual}(\mathbf{x}^v + \Delta \mathbf{x}) \approx \mathbf{h}_{nonVirtual}(\mathbf{x}^v) + H \Delta \mathbf{x} \quad (15)$$

$$\mathbf{g}(\mathbf{x}^v + \Delta \mathbf{x}) \approx \mathbf{g}(\mathbf{x}^v) + G \Delta \mathbf{x}$$

where, $H = \partial \mathbf{h}_{nonVirtual}(\mathbf{x}) / \partial \mathbf{x}$ and $G = \partial \mathbf{g}(\mathbf{x}) / \partial \mathbf{x}$.

Therefore, the necessary conditions for method of Lagrange multipliers are:

$$(\mathbf{h}_{nonVirtual}(\mathbf{x}^v) + H \Delta \mathbf{x} - \mathbf{z})^T W H + (\boldsymbol{\lambda}^v + \Delta \boldsymbol{\lambda}) G = 0 \quad (16)$$

$$\mathbf{g}(\mathbf{x}^v) + G \Delta \mathbf{x} = 0$$

Or

$$\begin{bmatrix} \Delta \mathbf{x} \\ \Delta \boldsymbol{\lambda} \end{bmatrix} = - \begin{bmatrix} H^T W H & G^T \\ G & 0 \end{bmatrix}^{-1} \begin{bmatrix} H^T W (\mathbf{h}_{nonVirtual}(\mathbf{x}^v) - \mathbf{z}) + G^T \boldsymbol{\lambda}^v \\ \mathbf{g}(\mathbf{x}^v) \end{bmatrix} \quad (17)$$

The solution is provided by the following iterative algorithm until convergence,

$$\begin{bmatrix} \mathbf{x}^{v+1} \\ \boldsymbol{\lambda}^{v+1} \end{bmatrix} = \begin{bmatrix} \mathbf{x}^v \\ \boldsymbol{\lambda}^v \end{bmatrix} - \begin{bmatrix} H^T W H & G^T \\ G & 0 \end{bmatrix}^{-1} \begin{bmatrix} H^T W (\mathbf{h}_{nonVirtual}(\mathbf{x}^v) - \mathbf{z}) + G^T \boldsymbol{\lambda}^v \\ \mathbf{g}(\mathbf{x}^v) \end{bmatrix} \quad (18)$$

The covariance matrix of the state and Lagrange multiplier is:

$$\text{Cov}(\mathbf{x}, \boldsymbol{\lambda}) = \begin{bmatrix} H^T W H & G^T \\ G & 0 \end{bmatrix}^{-1} \begin{bmatrix} H^T W^T H + G^T \boldsymbol{\lambda} \boldsymbol{\lambda}^T G & 0 \\ 0 & 0 \end{bmatrix} \begin{bmatrix} H^T W H & G^T \\ G & 0 \end{bmatrix}^{-T} \quad (19)$$

C. Protection Logic

Once the solution is calculated by equation (7) or (18), chi-square test is applied. Chi-square test quantifies the goodness of fit between the model and measurements by providing the probability that the measurements are consistent with the dynamic model of the protection zone. Chi-square test is applied as follows:

First the chi-square value ξ is computed:

$$\xi = \sum_{i=1}^n \left(\frac{h_i(\mathbf{x}) - z_i}{\sigma_i} \right)^2 \quad (20)$$

The probability (confidence level) that the measurements and the model fit together within the accuracy of the meters is computed from:

$$Pr[\chi^2 \geq \xi] = 1 - Pr[\chi^2 \leq \xi] = 1 - Pr(\xi, \nu) \quad (21)$$

where ν is the degree of freedom, which is the difference between the number of measurements and states.

A confidence level around 1.0 (small chi-square value) infers the measurements are highly consistent with the dynamic model, which means there is no internal abnormality. On the other hand, a confidence level around 0.0 (large chi-square value) infers the measurements do not fit with the dynamic model predicted values, which means this dynamic model of the protection zone has changed due to an internal abnormality. It indicates that some internal faults have changed the structure of the model, so the protective relay should take protection action and protect the zone from further damage. To avoid false tripping from transients, the result of the chi-square test is integrated over a user selected interval (one or two cycles) before a trip command is issued.

The overall framework of DSE-based protection is shown in Figure 2.

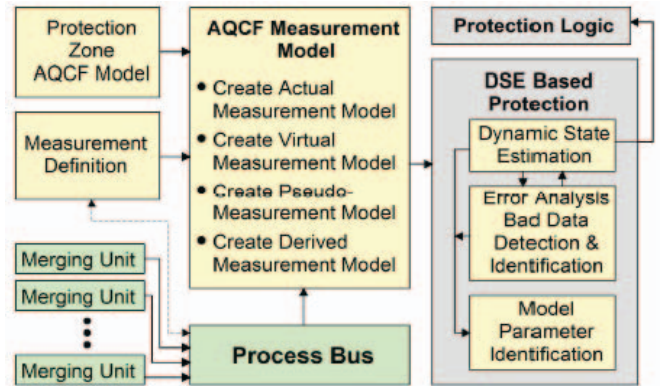


Figure 2. Framework of DSE-based protection

Note that the use of dynamic state estimation, which is a very powerful tool, can bring lots of benefits, e.g. bad data detection, parameter identification, etc.. Bad data detection

can detect hidden failures in the data acquisition system. In addition, parameter identification can be performed to obtain the protection zone dynamic model with higher fidelity which will result in more accurate state estimation results.

IV. NUMERICAL CASES

A 115kV, 48MVar three phase capacitor bank case is illustrated here. Both unconstraint WLS and CWLS methods are tested to compare the estimation results. The capacitor bank under protection is at the bottom of Figure 3.

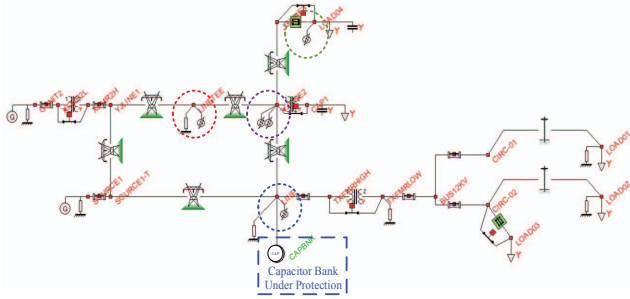


Figure 3. DSE-based protection test system

The configuration of the capacitor bank is shown in Figure 4.

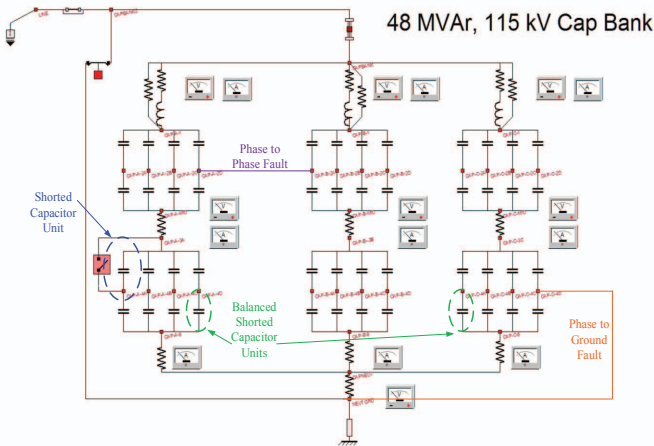


Figure 4. Configuration of the capacitor bank

Sixteen measurements are measured from the capacitor bank: three terminal currents, three phase-to-ground voltages, three midpoint currents, three midpoint-to-ground voltages, three bottom currents and one neutral to ground voltage. In general, we need a set of measurements that will make the capacitor bank observable. For this configuration of the capacitor bank, the minimum number of measurements is four to meet the observability criterion. The additional measurements provide redundancy.

A. Internal Fault

Several internal faults are simulated. For example, a fault causes one capacitor unit, shown in the blue circle in Figure 4, to be shorted at time 6.7s. This internal fault is used here to show the purposed protection results. The measurements from time span 6.640s to 6.740s are shown in Figure 5. Only three terminal currents and voltages are shown to save space.

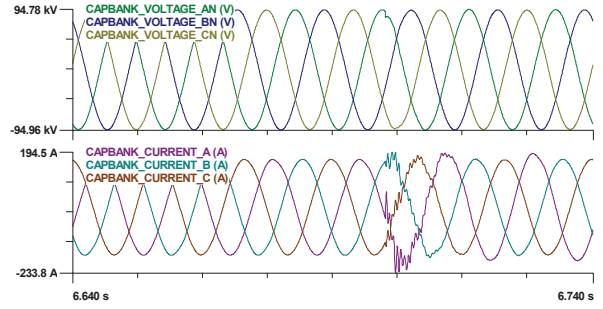


Figure 5. Measurements of the capacitor bank from 6.640s to 6.740s

Figure 6 and Figure 7 are the results of DSE-based protection using WLS and CWLS method respectively. The number showing in the middle of Y-axis for each channel is the average value of the samples between two cursors. It can be seen that before the internal fault happens (6.7s), which represents normal operating condition, the residual (errors) of phase AN voltage using CWLS is a little bit smaller than the residual using WLS. For the first virtual measurement residual, since it is treated as constraint in CWLS, the residual is zero in that case. The average square root of covariance using CWLS is also a little bit smaller than the WLS method, which means the CWLS results in more accurate estimated state values for the protection zone.

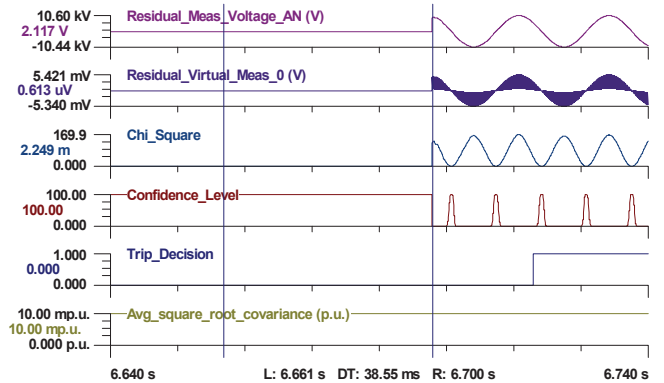


Figure 6. Protection results of DSE-based protection using unconstraint WLS

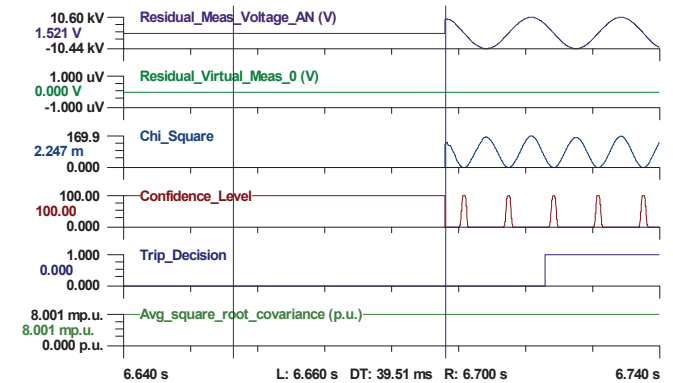


Figure 7. Protection results of DSE-based protection using CWLS

When the internal fault occurs, the confidence level drops to zero in both cases and the trip decision is issued after the confidence level keeping low for two cycles. From

engineering application aspect, the accuracy of both WLS and CWLS methods meet the protection requirements of dependability and security.

Due to space limitation, the results of the balanced shorted units case, the phase to phase fault case and the phase to ground fault case are not listed here. They all have similar results as the single shorted unit fault case.

B. External Fault

For the external faults, the DSE-based protection should not trip the capacitor bank (because the capacitor bank is still healthy). Several external faults are simulated as well. A capacitor bank terminal phase B to phase C fault (as shown in the blue circle in Figure 3) is illustrated here. The fault occurs at time 5.8s. The measurements from time span 5.740s to 5.840s are shown in Figure 8.

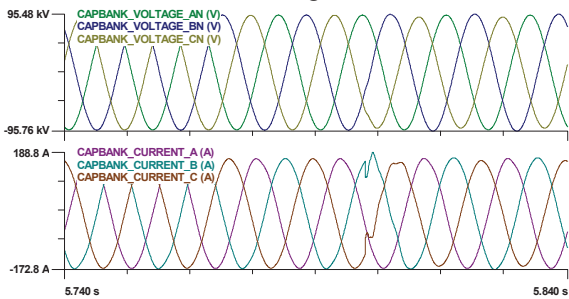


Figure 8. Measurements of the capacitor bank from 5.74s to 5.84s

Figure 9 and Figure 10 are the results of DSE-based protection using WLS and CWLS method respectively.

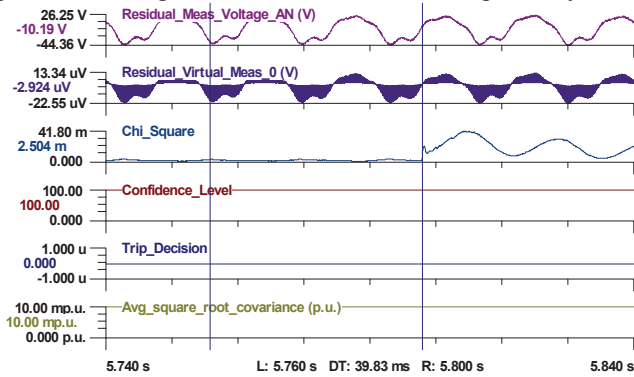


Figure 9. Protection results of DSE-based protection using unconstrained WLS

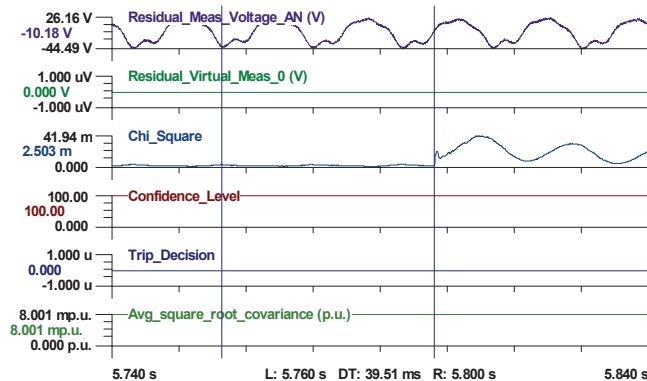


Figure 10. Protection results of DSE-based protection using CWLS

It can be seen that both WLS and CWLS DSE-based protection do not respond to the external fault, which proves the security of the proposed method.

V. CONCLUSIONS

This paper introduces a dynamic state estimation based protection for the capacitor bank, using the unconstrained (WLS) and constraint weighted least squares (CWLS) method, which treats the internal equations of the capacitor bank as constraints. The CWLS eliminates possible estimation errors caused by assumed low variance for virtual measurements. The comparison of constraint and unconstrained WLS method has been demonstrated. For most protection cases, the accuracy and sensitivity of both algorithms is high enough to provide secure and dependable protection.

ACKNOWLEDGMENT

This work is supported by PSERC and EPRI. Their support is greatly appreciated.

REFERENCES

- [1] "IEEE Guide for Application of Shunt Power Capacitors," *IEEE Std 1036-1992*, 1993.
- [2] M. Bishop, T. Day and A. Chaudhary, "A primer on capacitor bank protection," *IEEE Trans. Industry Applications*, vol.37, no.4, pp.1174,1179, Jul. 2001.
- [3] J. A. Zulaski, "Shunt Capacitor Bank Protection Methods," *IEEE Trans. Power Apparatus and Systems*, vol.PAS-101, no.6, pp.1305,1312, June 1982.
- [4] B. Richter, L. Gebhardt and J. Oliveira, "Overvoltage protection of capacitor banks," *2011 International Symposium on Lightning Protection*, pp.221-225, 3-7 Oct. 2011.
- [5] S.K. Buggaveeti and S.M. Brahma, "Improved Overcurrent Protection of Capacitor Banks Using Mathematical Morphology," *IEEE Trans. Power Delivery*, vol.26, no.3, pp.1972,1979, July 2011.
- [6] R. Moxley, J. Pope and J. Allen, "Capacitor bank protection for simple and complex configurations," *2012 65th Annual Conference for Protective Relay Engineers*, pp.436-441, 2-5 Apr. 2012.
- [7] D. L. Phillips, "A technique for the numerical solution of certain integral equations of the first kind," in *J. Assoc. Comput. Mach.*, vol. 9, pp. 97-101, 1962.
- [8] G.K. Stefopoulos, G.J. Cokkinides and A.P.S. Meliopoulos, "Quadratic integration method for transient simulation and harmonic analysis," in *2008 13th International Conference on Harmonics and Quality of Power*, pp.1-6, Sept. 2008.
- [9] R. Fan, A.P.S. Meliopoulos, G.J. Cokkinides, L. Sun and Y. Liu, "Dynamic state estimation-based protection of power transformers," in *2015 IEEE Power & Energy Society General Meeting*, pp.1-5, July 2015.
- [10] Y. Liu, A.P.S. Meliopoulos, R. Fan and L. Sun, "Dynamic State Estimation based protection of microgrid circuits," in *2015 IEEE Power & Energy Society General Meeting*, pp.1-5, July 2015.
- [11] A.P.S. Meliopoulos, L. Sun, R. Fan and P. Myrda, "Update on object-oriented DSE based protection," in *Fault and Disturbance Conference*, pp.1-5, Apr. 2014.